Journal of the Korean Chemical Society
2023, *Vol. 67, No. 6*
Printed in the Republic of Korea
https://doi.org/10.5012/jkcs.2023.67.6.415

Synthesis of Platinum-Reduced Graphene Oxide (Pt-rGO) Nanocomposite for Selective Detection of Hydrogen Peroxide as a Peroxidase-Mimic Catalyst

Doyun Park, Min Young Cho, and Kuan Soo Shin*
*Department of Chemistry, Soongsil University, Seoul 06978, Korea. *E-mail: kshin@ssu.ac.kr*
(Received October 24, 2023; Accepted November 27, 2023)

ABSTRACT. In this study, we report the one-pot synthesis of reduced graphene oxide (rGO) containing platinum nanoparticles with catalytic activity to break down hydrogen peroxide as a peroxidase-mimicking catalyst. A single reducing agent was used to reduce graphene oxide and a platinum precursor at a moderately low temperature of 70 ℃. The rGO was homogeneously decorated with platinum nanoparticles. The catalytic activity of Pt-rGO was investigated for the oxidation of 3,3',5,5'-tetramethylbenzidine (TMB), a peroxidase substrate, in the presence of hydrogen peroxide. The Pt-rGO coupled with glucose oxidase was also able to detect glucose at millimolar concentrations (up to 1 mM). Our results show that the Pt-rGO composite is a promising catalyst for the detection of hydrogen peroxide. This method was also applied for the detection of glucose.

Key words: Platinum nanoparticle, Graphene oxide, Hydrogen peroxide, Colorimetric detection, Glucose oxidation

INTRODUCTION

Graphene has a two-dimensional (2D) honeycomb lattice morphology that is tightly packed with a flat monolayer of carbon atoms. It has been extensively investigated because of its high surface area (approximately 2600 m^2g^{-1}), high conductivity, good mechanical strength, and flexibility.[1-2] Thus, graphene is a promising platform for adsorption of catalytically active metal nanoparticles, making it a good substructure for heterogeneous catalytic processes. Graphene, however, has wrinkles on its 2D surface owing to flaws, functional groups, and mechanical tensions.[3-4] Nanomaterials are mostly located at the site of the wrinkles on graphene oxide (GO).[5] GO can be reduced using hydrazine as a reducing agent.[6] Metallic nanoparticles (NPs) such as copper and platinum have also been synthesized using hydrazine with a capping agent to protect them from oxidation.[7]

Enzymes are biological catalysts that have been widely applied in various industrial fields. As natural enzymes are very sensitive to temperature and pH, they are catalytically active in a narrow range of temperature and pH. In the past two decades, many efforts have been made to develop a novel mimetic enzyme using NPs.[8-12] NPs have a large surface-to-volume ratio and can demonstrate highly efficient catalytic activity.[13-15] Stable metallic NPs are vulnerable to oxidation in the air. Reduced GO sheets prepared with metallic NPs are generally stable enough to prevent oxidation. In a previous study, we developed a stable Cu-rGO composite using a single-step synthesis.[16] In addition, we also analyzed the intrinsic peroxidase-like catalytic activity to oxidize 3,3',5,5'-tetramethylbenzidine (TMB), a peroxidase substrate, in the presence of hydrogen peroxide (H_2O_2).[16] The catalytic activity of Cu-rGO was applied for the colorimetric detection of glucose.[16] In the current study, we used platinum (Pt), which is widely used as a catalyst in chemical industries. Although bulk Pt is not chemically active, Pt nanomaterials are important catalysts.[17-19] In this study, we synthesized a stable Pt-rGO composite using a single reducing agent in a single-step reaction. We also analyzed the catalytic activity for the oxidation of TMB in the presence of H_2O_2 to measure the absorbance at 652 nm. Interestingly, Pt-rGO had a higher signal-to-noise ratio at the same concentration of H_2O_2 than Cu-rGO within 10 s. Furthermore, Pt-rGO coupled with glucose oxidase showed a linear increase in absorbance with millimolar concentrations of glucose (up to 1 mM). As Pt is a versatile catalyst in industry, our system could have many potential applications in a wide range of fields.

EXPERIMENTAL

Reagents and Materials

All chemicals were purchased from Sigma-Aldrich (St. Louis, MO, USA), and Milli-Q water (18.2 MΩ cm) was used for the preparation of all the reagents.

Synthesis of Pt-rGO Composite and rGO

Graphene oxide (GO) was prepared by the improved Hummers' method. The protocol has been previously reported elsewhere.[16,20-21] After synthesizing of GO, 20 mg of GO resuspended in 10 ml of Milli-Q water was stirred with 175.6 μL of 8% (w/v) hexachloroplatinic acid solution (H_2PtCl_6) for 30 to 60 min. Sodium hydroxide (0.5 M) was added to the mixture, which was heated at 70 ℃ for 5 min. Hydrazine hydrate solution (60–80%, 300 μL) was added into the reaction mixture after it was cooled down to room temperature. The mixture was further stirred for 40 min. Excess Pt particles in the solution were removed by iterative centrifugation and the Pt-rGO composite was washed using ethanol. rGO was synthesized using the same procedure except for the platinum compound.

Material Characterization

Fourier-transform infrared (FT-IR) spectra were obtained using a Thermo Scientific Nicolet 6700 spectrophotometer, and UV-VIS absorption spectra were measured using an Avantes Avaspec-3648 spectrophotometer. The temperature of the cuvette was maintained using a refrigerated circulating bath. Transmission electron microscopy (TEM) images were obtained using a JEM-F200 from JEOL, and scanning electron microscopy (SEM) images were recorded using a LIBRA 120 microscope (Zeiss). X-ray diffraction (XRD) analysis was performed using a D2 PHASER from Bruker with Cu Ka radiation (1.5412 Å), and X-ray photoelectron spectroscopy (XPS) was performed using a Thermo Fisher Scientific K-alpha$^+$ X-ray.

Glucose Detection Assay

The glucose detection assay was carried out in two steps. An initial reaction mixture containing 200 μL of 10 mM phosphate buffer (pH 7.4), 20 μL of glucose oxidase (20 mg/ml), and 100 μL of glucose was incubated at 37 ℃ for 15 min. The reaction mixture was transferred into another vial containing 200 μL of 12 mM 3,3'5,5'-tetramethylbenzidine (TMB), and 2.7 mL of 0.5 M sodium acetate buffer (pH 3.8). After adding 30 μL of Pt-rGO, the vial was incubated at 60 ℃ for 3 min and cooled down to room temperature. The final solution was transferred into a cuvette, and the absorbance was measured at 652 nm. Lactose, fructose, and maltose (500 μM) were used in the control experiments.

RESULTS AND DISCUSSION

Synthesis and Characterization of Pt-rGO Composite

Pt-rGO was synthesized through a single-step reaction using hydrazine as a reducing agent. First, the morphology of Pt-rGO was investigated by SEM and TEM (*Fig.* 1).

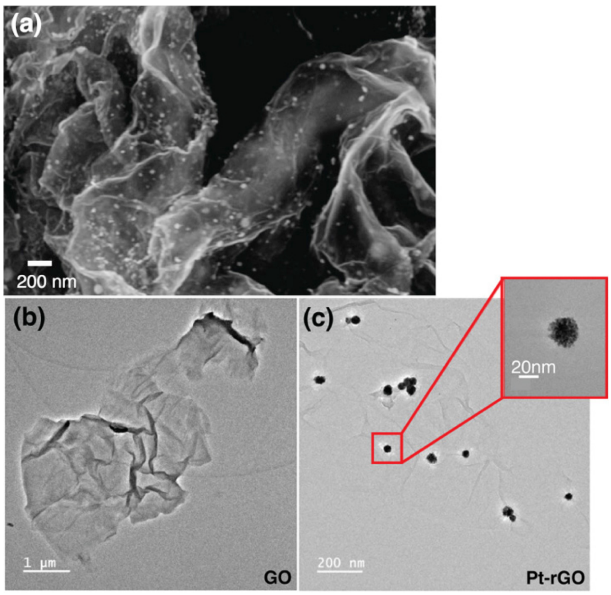

***Figure* 1.** Electron microscopy images. (a) SEM image of Pt-rGO and TEM images of (b) GO, (c) Pt-rGO.

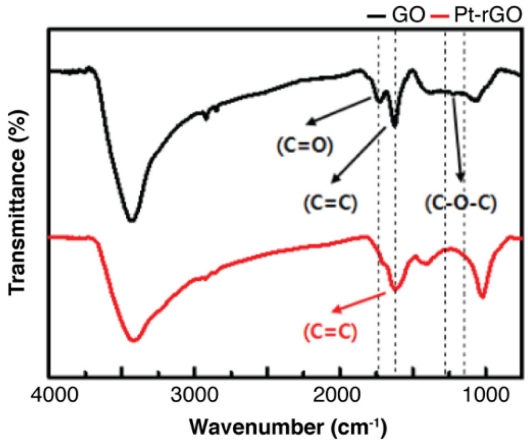

***Figure* 2.** FT-IR spectra of GO (black) and Pt-rGO (red).

The images indicate a well-distributed Pt nanoparticles (NPs) on the multilayered structure of the GO. The as-synthesized NPs are mostly spherical with an average size of 21.7±8.8 nm. Pt-rGO and GO were also analyzed by FT-IR to characterize the oxygen functional groups on the surface of the GO (*Fig.* 2).

The efficiency of the reduction of Pt-rGO by hydrazine is indicated by the functional groups detected. The two peaks at 3450 and 1050 cm^{-1} indicate the presence of adsorbed water molecules. The main features of the spec-

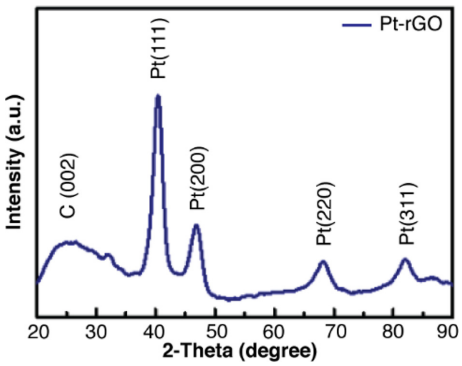

***Figure* 3.** XRD pattern of Pt-rGO.

tra are as follows: 3450 (O-H stretching vibration), 1726 (C=O stretching vibration from carbonyl and carboxyl groups), 1628 (aromatic C=C or absorbed water), and 1233 cm^{-1} (C-O-C of epoxy groups). The FT-IR spectra clearly indicate the chemical reduction of Pt-rGO, which has a smaller number of carbonyls, and epoxy groups. Pt-rGO was further analyzed by XRD and XPS.

Fig. 3 shows the XRD pattern of the Pt NPs on the rGO surface, with the characteristic crystallin Pt face-centered cubic phase distinguished by peaks corresponding to the (111), (200), (220), and (311) planes at 2θ values of 40.5°, 46.8°, 68.1°, and 81.2°, respectively. A broad peak at 25.0 corresponds to the (002) crystal plane of rGO (*Fig.* 3).

The electronic structure and chemical properties of Pt-rGO were analyzed using XPS (*Fig.* 4). The C 1s XPS spectrum of Pt-rGO shows three peaks corresponding to carbon atoms in different functional groups: the non-oxygenated ring C (284.7 eV), carbonyl groups (286.8 eV) and a peak at 288.3 eV indicating O-C=O groups. Notably, the peak for the carbonyl groups in Pt-rGO decreased significantly compared to that for GO. Furthermore, the Pt 4f XPS spectrum shows two distinct peaks at 71.2 eV and 74.5 eV corresponding to Pt $4f_{7/2}$ and Pt $4f_{5/2}$, respectively. Taken together, the results indicate that GO and Pt were reduced by hydrazine, and Pt NPs were formed homogeneously on the surface of rGO.

Pt-rGO as a Peroxidase Mimic Catalyst

Glucose oxidase (EC 1.1.3.4, GOx) catalyzes the oxidation of β-D-glucose to form β-D-gluconic acid and hydrogen peroxide (H_2O_2), The amount of glucose was quantitatively determined by the amount of hydrogen peroxide generated by GOx. Horseradish peroxidase (HRP) was used to catalyze and detect H_2O_2. After the chromo-

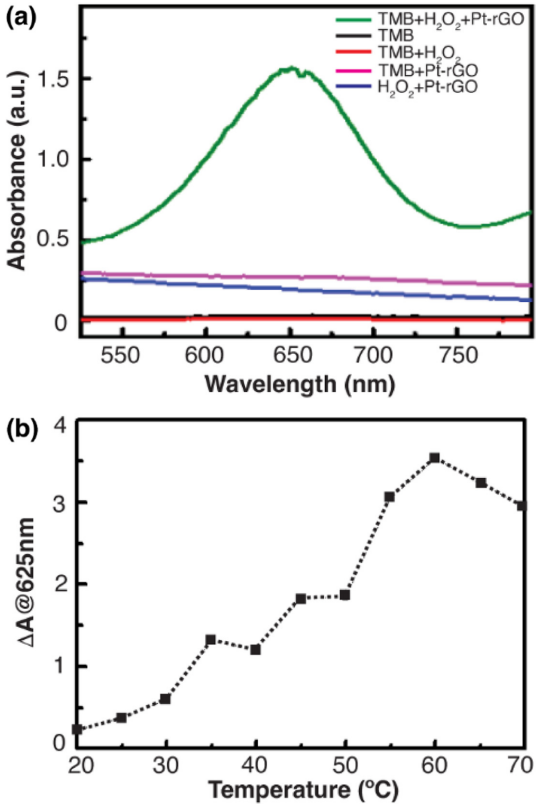

Figure 5. (a) UV-VIS absorption spectra. (b) temperature-dependent assay of Pt-rGO.

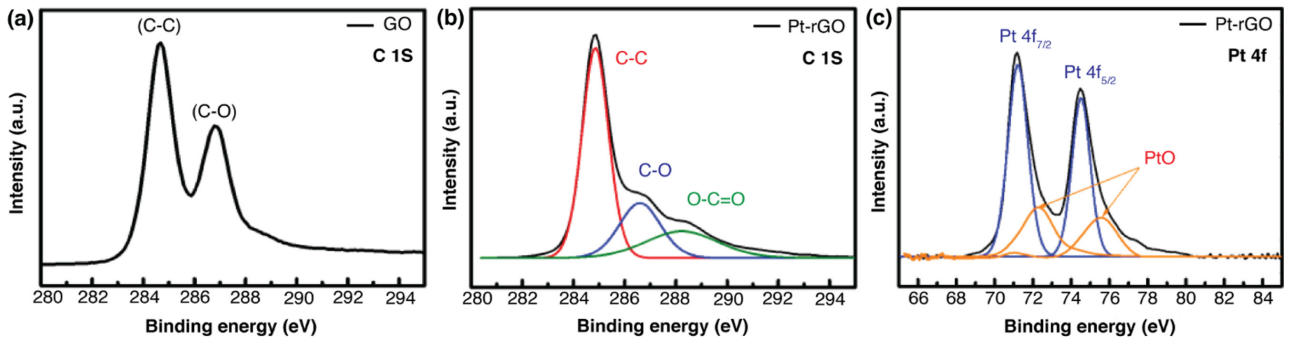

***Figure* 4.** XPS spectra of (a) C 1s for GO, (b) C 1s for Pt-rGO, and (c) Pt 4f for Pt-rGO.

genic substrate 3,3',5,5'-tetramethylbenzidine (TMB) is oxidized by HRP in the presence of H_2O_2, it has a specific absorption at 652 nm. The catalytic activity of our Pt-rGO composite was evaluated using TMB as a substrate for HRP. Various combinations of substrates, such as only TMB, TMB + H_2O_2, Pt-rGO + H_2O_2, Pt-rGO + TMB, and Pt-rGO + TMB + H_2O_2, were analyzed (*Fig.* 5a). A specific absorption peak was observed only in the vials containing Pt-rGO, TMB, and H_2O_2. Furthermore, the catalytic activity of Pt-rGO as an inorganic peroxidase mimic was estimated in the temperature range 20–70 ℃ (*Fig.* 5b). Interestingly, Pt-rGO retained its catalytic activity up to 70 ℃ and showed the maximum performance at 60 ℃. Natural peroxidases are generally denatured at that temperature.

Application for Glucose Detection at the Millimolar Concentrations

The catalytic activity of Pt-rGO was compared with that of Cu-rGO, which was synthesized and characterized in our prior study.[16] The catalytic activity of Pt-rGO is much higher than that of Cu-rGO (*Fig.* 6a). Notably, the signal-to-noise ratio of Pt-rGO increased rapidly within 10 s. This implies that the reduction of Pt is far faster than that of Cu. To validate Pt-rGO as a sensor for glucose, the limit of detection was analyzed by an assay at various concentrations of H_2O_2 from 1 mM to 100 mM (*Fig.* 6b). The linear increase in absorption at 652 nm indicates that Pt-rGO is a valid catalyst in the given range of H_2O_2 concentrations. Our system was further applied to detect H_2O_2 generated by the oxidation of glucose by GOx. As GOx is denatured at pH 4, the assay was performed in a stepwise manner. The initial reaction is the oxidation of glucose to gluconic acid and H_2O_2 by GOx. Subsequently, H_2O_2 was analyzed quantitatively using TMB and Pt-rGO composites at pH 4. A linear plot was obtained for the absorbance vs. concentration (from 1 to 20 mM) of glucose (*Fig.* 6c). The assay implies

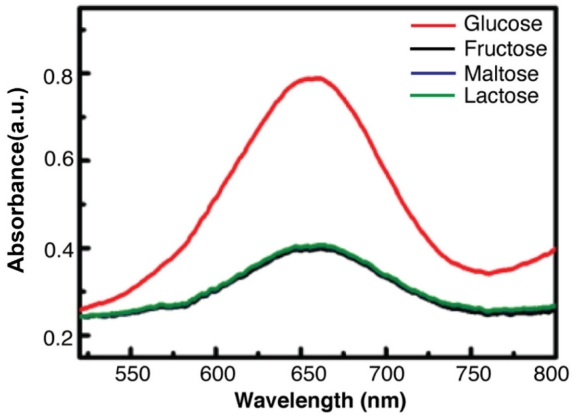

***Figure* 7.** UV-Vis absorption spectra indicate specificity for glucose compared to its analogs such as fructose, maltose, and lactose.

that our system can detect the glucose at the physiological concentration of a diabetic person. Our system was also evaluated with its analogs such as fructose, maltose, and lactose to check specificity (*Fig.* 7). The glucose oxidase enzymatic process demonstrates a notable specificity in oxidizing glucose compared to fructose, maltose, and lactose. The absorbance of glucose was dominant among the analogs. This implies that our system has good affinity for glucose.

CONCLUSION

The Pt-rGO composite was successfully synthesized by a single reaction at a relatively low temperature. Material analysis indicated that Pt NPs were homogeneously distributed on the surface of rGO. rGO sheets act as a support as well as a protective shell to prevent the oxidation of Pt NPs. The as-synthesized Pt-rGO hybrid catalyst showed high sensitivity and selectivity toward H_2O_2. Our hybrid catalyst was also used to detect the millimolar concentrations of glucose.

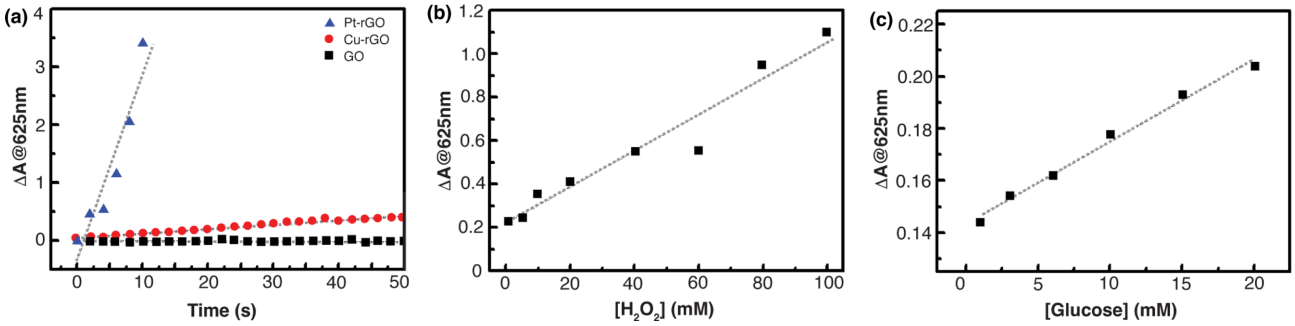

***Figure* 6.** (a) Time-dependent assay of GO, Cu-rGO, and Pt-rGO. Regression analysis shows that the relative absorbance at 625 nm is linearly related to the concentration of b) hydrogen peroxide (H_2O_2) and (c) glucose using Pt-rGO catalyst.

Acknowledgments. This work was supported by Basic Science Research Program of the National Research Foundation of Korea (NRF) (2018R1A2B6007742).

REFERENCES

1. Meyer, J. C.; Geim, A. K.; Katsnelson, M. I.; Novoselov, K. S.; Booth, T. J.; Roth, S. *Nature* **2007**, *446*, 60.
2. Guo, F.; Creighton, M.; Chen, Y.; Hurt, R.; Kulaots, I. *Carbon* **2014**, *66*, 476.
3. Deng, S.; Berry, V. *Materials Today* **2016**, *19*, 197.
4. Wang, C.; Liu, Y.; Lan, L.; Tan, H. *Nanoscale* **2013**, *5*, 4454.
5. Ruffino, F.; Giannazzo, F. *Crystals* **2017**, *7*.
6. Park, S.; An, J.; Potts, J. R.; Velamakanni, A.; Murali, S.; Ruoff, R. S. *Carbon* **2011**, *49*, 3019.
7. Wang, Y.; Asefa, T. *Langmuir* **2010**, *26*, 7469.
8. Wei, H.; Wang, E. *Chem Soc Rev* **2013**, *42*, 6060.
9. Su, Z.; Shen, H.; Wang, H.; Wang, J.; Li, J.; Nienhaus, G. U.; Shang, L.; Wei, G. *Advanced Functional Materials* **2015**, *25*, 5472.
10. Cheng, H.; Zhang, L.; He, J.; Guo, W.; Zhou, Z.; Zhang, X.; Nie, S.; Wei, H. *Anal Chem* **2016**, *88*, 5489.
11. Cheng, H.; Lin, S.; Muhammad, F.; Lin, Y.-W.; Wei, H. *ACS Sensors* **2016**, *1*, 1336.
12. Gao, L.; Yan, X. *Sci China Life Sci* **2016**, *59*, 400.
13. Vaccaro, B. J.; Clarkson, S. M.; Holden, J. F.; Lee, D. W.; Wu, C. H.; Poole Ii, F. L.; Cotelesage, J. J. H.; Hackett, M. J.; Mohebbi, S.; Sun, J.; Li, H.; Johnson, M. K.; George, G. N.; Adams, M. W. W. *Nat Commun* **2017**, *8*, 16110.
14. Mancin, F.; Prins, L. J.; Pengo, P.; Pasquato, L.; Tecilla, P.; Scrimin, P. *Molecules* **2016**, *21*.
15. Wang, X.; Hu, Y.; Wei, H. *Inorganic Chemistry Frontiers* **2016**, *3*, 41.
16. Kim, K.; Chaudhari, K. N.; Kim, S.; Kim, Y.; Shin, K. S. *Journal of Industrial and Engineering Chemistry* **2021**, *95*, 388.
17. Chen, A.; Holt-Hindle, P. *Chem Rev* **2010**, *110*, 3767.
18. Wei, G.; Zhang, Y.; Steckbeck, S.; Su, Z. Q.; Li, Z. *Journal of Materials Chemistry* **2012**, *22*, 17190.
19. Zhang, P. P.; Zhao, X. N.; Zhang, X.; Lai, Y.; Wang, X. T.; Li, J. F.; Wei, G.; Su, Z. Q. *ACS Applied Materials & Interfaces* **2014**, *6*, 7563.
20. Akhavan, O.; Ghaderi, E.; Aghayee, S.; Fereydooni, Y.; Talebi, A. *Journal of Materials Chemistry* **2012**, *22*.
21. Esfandiar, A.; Akhavan, O.; Irajizad, A. *Journal of Materials Chemistry* **2011**, *21*.